

O. Hahtela, P. Sievilä, N. Chekurov and I. Tittonen, Atomic layer deposited alumina (Al_2O_3) thin films on a high- Q mechanical silicon oscillator, Journal of Micromechanics and Microengineering 17, 737-742 (2007).

© 2007 Institute of Physics Publishing

Reprinted with permission.

<http://www.iop.org/journals/jmm>

Atomic layer deposited alumina (Al_2O_3) thin films on a high- Q mechanical silicon oscillator

O Hahtela^{1,2}, P Sievilä^{1,2}, N Chekurov^{1,2} and I Tittonen^{1,2}

¹ Micro and Nanosciences, Micronova, Helsinki University of Technology, PO Box 3500, FIN-02015 TKK, Finland

² Center for New Materials, Helsinki University of Technology, Finland

E-mail: ossi.hahtela@tkk.fi

Received 17 October 2006, in final form 21 December 2006

Published 8 March 2007

Online at stacks.iop.org/JMM/17/737

Abstract

In this paper, the influence of the atomic layer deposited alumina (Al_2O_3) thin films on the dynamics of a high- Q mechanical silicon oscillator was experimentally studied. The resonance frequency and Q value of uncoated oscillators used in this work were about $f_0 = 27$ kHz and $Q = 100\,000$ at $p < 10^{-2}$ mbar and $T = 300$ K. Deposited alumina film thicknesses varied from 5 to 662 nm. It is demonstrated that the resonance frequency of the mechanical oscillator increases with the film thickness because the added alumina films effectively stiffen the oscillator structure. In addition, it is shown that alumina thin films with thickness up to 100 nm can be deposited on microfabricated mechanical resonant structures without degrading the initially high quality (Q value) of the resonance. The resonance frequency of the silicon oscillator was less sensitive to the changes in ambient temperature with thicker alumina coatings. The reflectivity of silicon at 633 nm was reduced from $R_{\text{Si}} = 0.35$ to $R_{\text{AR}} = 0.035$ by coating the silicon oscillator with an alumina film whose thickness corresponds to the quarter of the optical wavelength serving as a single-layer anti-reflection coating.

1. Introduction

Thin film-coated microelectromechanical systems (MEMS) are increasingly utilized in a vast variety of mechanical, electrical and optical device applications [1–4]. Alumina (Al_2O_3) has many favorable properties when used as thin film coatings of MEMS devices. Alumina is a hard and stiff material with a high Young's modulus [5]. It has good thermal and chemical stability and firm adhesion to many surfaces [6, 7]. Alumina can also be used under high temperature and harsh environments. In addition, alumina has high dielectric constant and excellent insulating properties [7, 8]. Surface effects have an important and dominant role due to the typically small size and large surface-to-volume ratio of MEMS devices. Many surface-related issues such as friction, wear, adhesion, oxidation and short circuiting can cause malfunction or impair the performance, reliability and durability of the devices. Protective alumina thin film coatings can be used to minimize or prevent such problems

[1–3, 9]. Alumina is optically transparent over a wide range of wavelengths [10], and it can be used as a low refractive index material [11] in optical coatings and multilayer stacks such as AR and HR coatings, polarizers and filters.

Atomic layer deposition (ALD) is based on sequential self-limiting surface reactions. Thus, the deposited film thickness can be controlled at the atomic level. Growing of the film is extremely linear and directly proportional to the number of individual deposition cycles [11, 12]. ALD is an especially convenient technique to deposit uniform and conformal thin films on MEMS devices because they typically involve complex structures with small gaps, high aspect ratio trenches and shaded areas. ALD films are typically very flat, and the surface quality is extremely good. In addition, the ALD technique allows film deposition at modest or low temperatures (35–500 °C) [2, 11] if compared to other chemical vapor deposition (CVD) techniques.

The motivation for this work is to study possibilities of depositing thin films on resonant micromechanical structures

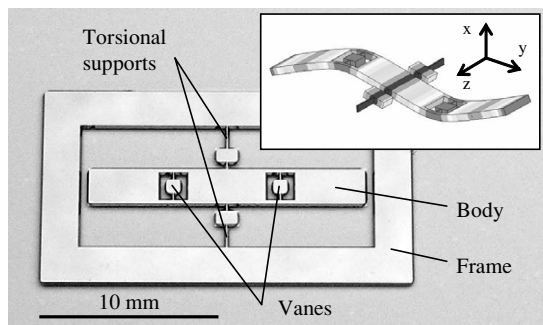


Figure 1. A photograph of the non-tilting out-of-plane mode high- Q mechanical silicon oscillator. The sizes of each rectangular vane and oscillator body are $0.8 \times 0.8 \times 0.38 \text{ mm}^3$ and $1.5 \times 14 \times 0.38 \text{ mm}^3$, respectively. The inset shows the vibrational mode pattern of the high- Q mode oscillation.

without degrading the initially high mechanical quality (Q value) of the resonance. This is of great importance when depositing functional, protective or optical thin films on sensitive MEMS devices. This paper concentrates on studying the effects of amorphous ALD alumina thin films on the performance of high- Q mechanical silicon oscillators.

2. High- Q mechanical silicon oscillator

The high- Q mechanical silicon oscillator used in this work is illustrated in figure 1. This non-tilting out-of-plane mode oscillator design was first presented in [13]. The uncoated oscillators have a resonance frequency of about $f_0 = 27 \text{ kHz}$, and the highest measured Q values exceed 100 000 at low pressure ($p < 10^{-2} \text{ mbar}$) and at room temperature. The inset in figure 1 shows the result of the finite element method (FEM) simulation [13] of the high- Q mode pattern which basically corresponds to the second flexural mode of a free-free beam. Oscillators were fabricated from double-sided polished, $380 \mu\text{m}$ thick (100) oriented single-crystal silicon wafers (p-type, $5\text{--}10 \Omega \text{ cm}$). A thermally grown silicon dioxide layer, which was patterned using double-sided UV lithography, served as an etch mask. The oscillator structures were released by using double-sided anisotropic wet etching in a 25% tetramethyl ammonium hydroxide (TMAH) solution at $85 \text{ }^\circ\text{C}$. A detailed discussion of the non-tilting out-of-plane mode oscillator can be found in [13].

3. Atomic layer deposition of alumina

Silicon oscillators were coated with alumina thin films by using the ALD technique with trimethyl aluminum ($\text{Al}(\text{CH}_3)_3$, TMA) and water as precursors³ [14, 15]. The binary self-limiting chemical reactions between the gas phase precursor molecules and a solid surface that define the Al_2O_3 growth on the substrate are



³ In this work, the alumina films were deposited using a Beneq TFS 500 ALD reactor.

where the asterisks represent the surface species. Each AB growth cycle consists of sequential exposure to TMA and H_2O . When TMA is introduced to the ALD reactor, it starts to react with the hydroxyl ($-\text{OH}$) groups on the substrate surface. When this surface reaction has completed, the remaining reactants and by-products are purged from the reactor. In the next step, H_2O vapor is introduced to the reactor. H_2O reacts with the methyl ($-\text{CH}_3$) groups on the surface until all the $-\text{OH}$ groups have become regenerated. This is followed by another purging step after which the surface is ready for a new AB cycle. By repeating these AB cycles, a desired film thickness can be achieved.

The precursors were introduced to the ALD reactor using N_2 as a carrier gas. The deposition temperature and pressure in the ALD reactor were $T_{\text{ALD}} = 220 \text{ }^\circ\text{C}$ and $p_{\text{ALD}} = 2.3 \text{ mbar}$, respectively. The growth rate of alumina was 0.09 nm/cycle and the duration of each AB cycle was 2 s . Deposited film thicknesses varied from 5 to 662 nm . The film thicknesses were determined by ellipsometry. The refractive index of ALD alumina thin films varies slightly as a function of the deposition temperature [11]. In our case, with a deposition temperature of $220 \text{ }^\circ\text{C}$, the ellipsometrically determined refractive index for alumina films was $n = 1.64$ at a HeNe-laser wavelength of $\lambda = 633 \text{ nm}$.

4. Measurements and results

4.1. Frequency response of the silicon oscillator

Dynamic characteristics of the uncoated and alumina-coated oscillators were measured by using an optical beam deflection technique [16]. First, the silicon oscillator was mechanically excited by a piezo-actuator which was attached to the oscillator mount. A HeNe-laser beam was focused on the center of the oscillator body. The deflection of the laser beam reflected off the oscillator top surface was detected by a segmented, position-sensitive photodiode. The oscillation amplitude and phase were determined by monitoring the photodiode output with a lock-in amplifier.

Figure 2 shows a typical response of a mechanical silicon oscillator when the piezo-excitation frequency is swept over the mechanical resonance. In this case, the oscillator had a 100 nm thick alumina coating. The Lorentzian fit of the measured oscillation amplitude indicates high linearity and purity of the resonance when a moderate excitation level is used. The width of the resonance is $\Delta f = f_0/Q = 270 \text{ mHz}$. However, the spectral resolution in our measurements is even much better. It was possible to determine the position of the resonance peak maximum with an accuracy of 10 mHz . Therefore, even the ppm level changes in the resonance frequency could be easily detected.

4.2. Resonance frequency as a function of alumina film thickness

In order to estimate the influence of the alumina thin films on the resonance frequency, we model our silicon oscillator as a uniform beam with a rectangular cross-section. In addition, because the length L of the oscillator body is much larger than the width w and thickness h (i.e. $L \gg w$ and $L \gg h$), the resonance frequency of the n th flexural mode can be

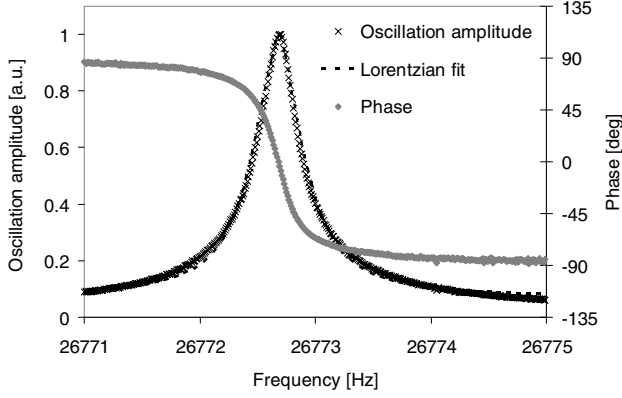


Figure 2. Normalized frequency responses of the oscillation amplitude and phase at $p = 0.1$ mbar and $T = 297$ K. The silicon oscillator was coated with a 100 nm thick alumina layer. The Lorentzian fit of the measured oscillation amplitude indicates highly linear and pure resonance when a moderate excitation level is used.

determined according to the Euler–Bernoulli beam theorem [17] by

$$f_0 = \frac{(\beta_n L)^2}{2\pi} \frac{h}{L^2} \sqrt{\frac{E_S}{12\rho_S}}, \quad (1)$$

where E_S and ρ_S are Young's modulus and density of silicon, respectively. The parameter $\beta_n L$ is related to the n th flexural mode. For the second flexural mode of the free–free beam $\beta_2 L = 7.8532$. If the silicon oscillator is coated on all sides with a thin uniform alumina film of thickness t , the resonance frequency can be approximated by transforming equation (1) to [18]

$$f_c = \frac{(\beta_n L)^2}{2\pi} \frac{h}{L^2} \sqrt{\frac{E_S \frac{wh}{12} + E_A \left(\frac{w}{2} + \frac{h}{6}\right)t}{\rho_S wh + 2\rho_A (w+h)t}}, \quad (2)$$

where L , w and h are the length, width and thickness of the uncoated oscillator body, respectively. E_A and ρ_A are Young's modulus and density of the ALD alumina, respectively. The size and material parameters for our silicon oscillator are $L = 14$ mm, $w = 1.5$ mm, $h = 380$ μ m, $E_S = 150$ GPa [19] and $\rho_S = 2330$ kg m⁻³. The density of the ALD alumina depends on the growth process parameters and is of the order of $\rho_A = 3500$ kg m⁻³ [7].

The resonance frequencies of the alumina-coated silicon oscillators were measured as a function of alumina film thickness (figure 3). The increase in the resonance frequency is very linear when the film thickness is small compared to the thickness of the silicon oscillator. According to a statistical analysis, the dependence of the resonance frequency on the alumina film thickness was 5.18 ± 0.04 ppm nm⁻¹. This small uncertainty implies that the thickness of the alumina thin film can be determined with a very high accuracy. For example, the statistical uncertainty in the thickness measurement of a 1 nm thick film would be of the order of one-tenth of the thickness of an alumina monolayer. However, the finite reading accuracy (10 mHz) of a single resonance frequency measurement introduces uncertainty in the determination of the film thickness that is comparable to one monolayer.

Young's modulus of the ALD alumina was determined to be $E_A = 177$ GPa by fitting equation (2) on the experimental

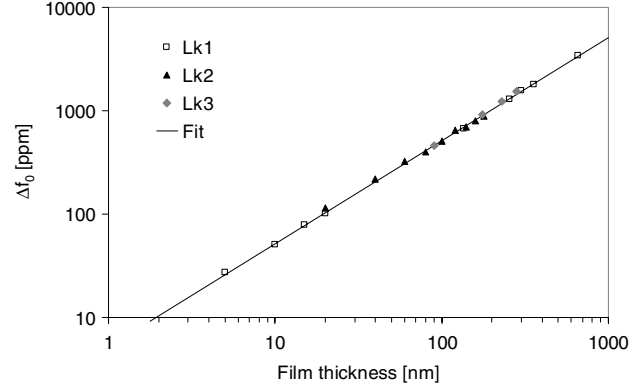


Figure 3. Change in the resonance frequency as a function of alumina film thickness. The dependence of the resonance frequency on the alumina film thickness is 5.18 ppm nm⁻¹. Three silicon oscillators (Lk1, Lk2 and Lk3) with various alumina film thicknesses were used. The solid line shows a fitting according to equation (2), yielding Young's modulus of ALD alumina of $E_A = 177$ GPa.

data of f_c with variable film thickness. It should be noted that our silicon oscillator is not a totally ideal uniform beam with rectangular cross-sections because the sidewalls are oblique due to anisotropic wet etching, and the openings around the vanes introduce local decrease in the effective stiffness of the oscillator body [13]. However, this experimentally obtained value for Young's modulus for the ALD alumina is in a good agreement with other values reported in earlier experiments ($E_A = 168$ – 182 GPa [5]).

4.3. *Q* value as a function of alumina film thickness

The *Q* value of a mechanical resonant system is defined as $Q = 2\pi E_0/\Delta E$, where E_0 is the stored vibrational energy and ΔE is the total energy loss per cycle of vibration. The total energy loss per cycle is a sum of various loss sources and the total *Q* value can be derived from

$$\frac{1}{Q} = \frac{1}{Q_i} + \frac{1}{Q_s} + \frac{1}{Q_v}, \quad (3)$$

where Q_i is determined by the internal losses, Q_s is related to energy losses through the oscillator support structure (clamping losses) and Q_v is due to the viscous and acoustic losses to the surrounding medium. Internal losses result e.g. from thermoelastic dissipation, motion of lattice defects, phonon–phonon scattering, surface effects, etc [20].

We measured the *Q* value of the silicon oscillator as a function of alumina film thickness (figure 4). Our measurements were performed at low pressure ($p < 10^{-2}$ mbar) so that the effects of viscous damping ($1/Q_v$) can be neglected. Alumina films with thicknesses up to 100 nm had no significant influence on the *Q* value of the mechanical resonance. This was rather unexpected because earlier experiments have shown that mechanical quality of balanced and low loss high-*Q* structures is very sensitive to additional deposited films on the device [21–23]. Our measurements imply that ALD alumina itself has low internal friction and is thus a potential choice of material for high-*Q* devices. Another reason for the low losses introduced by very thin alumina films is the fact that the ALD technique allows

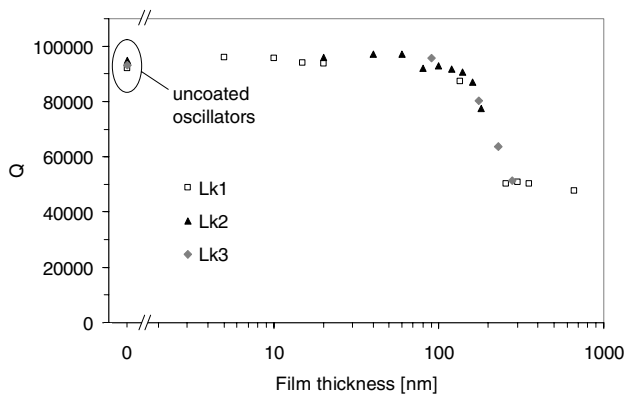


Figure 4. Q value measured as a function of the alumina film thickness at $p < 10^{-2}$ mbar and $T = 297$ K. Three oscillators (Lk1, Lk2 and Lk3) with various film thicknesses were used.

for the film growth at low temperatures meaning that thermo-mechanical-based stress is low at the film-substrate boundary.

In order to minimize the clamping losses ($1/Q_s$) in our oscillator design, the torsional support beams were situated at the central nodal point of the oscillator body (figure 1). Ideally, the suspension bars experience only torsional motion in the high- Q mode oscillation. The dimensions of the torsional supports are chosen to correspond to the effective quarter wavelength of the resonance frequency of the oscillator body. Thus, the suspension bars act as impedance-matched acoustic transmission lines and the oscillator body experiences minimum energy dissipation through the support [19]. The additional ALD alumina thin films change the resonance frequency of the oscillator body. This results in impedance mismatch at the torsional supports leading to losses of mechanical energy. In our case, it seems that the impedance mismatch starts to impair the Q value when the alumina film thickness exceeds about 100 nm. For alumina films with thicknesses from 250 to 662 nm, the Q value was saturated to the level of 50 000. Although the influence of the deposited thin films on the Q value requires a more detailed study, we can conclude that it is possible to deposit dielectric thin films on micromechanical resonant structures without impairing the initially high quality of the corresponding mechanical resonances.

4.4. Temperature dependence of the resonance frequency

For most sensor applications, the temperature dependence of the resonance frequency should be as low as possible. Silicon has a negative temperature coefficient of Young's modulus which is the dominating factor in the temperature dependence of the resonance frequency of flexural mode silicon oscillators [24, 25].

Figure 5 shows the change in the resonance frequency as a function of ambient temperature for an uncoated silicon oscillator and for alumina-coated oscillators with film thicknesses of 100 nm, 253 nm and 662 nm. In this work, the ambient temperature was measured and controlled with a Pt100 resistor and a thermoelectric cooler (TEC). The uncertainty in temperature during the measurements was less than ± 0.25 K, which corresponds to the thermal drift of ± 0.23 Hz in the resonance frequency. For the uncoated

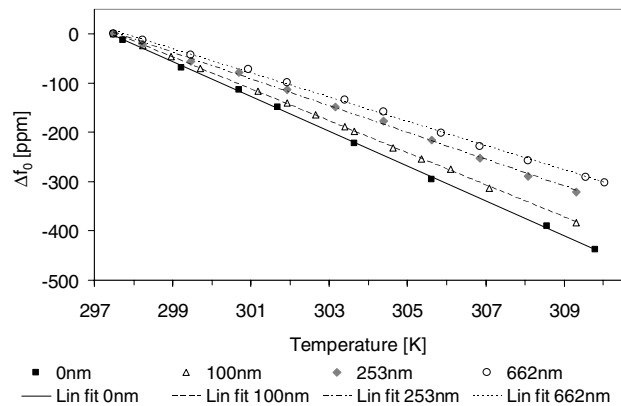


Figure 5. Resonance frequency as a function of the ambient temperature for an uncoated silicon oscillator and for alumina-coated oscillators with film thicknesses of 100 nm, 253 nm and 662 nm. The added lines show linear fittings to the measurements.

oscillator, the thermal drift in resonance frequency was measured to be -35 ppm K^{-1} . Using this value and equation (1), where Young's modulus E_S is replaced with a linear approximation $E_S = E_{S0}(1 + \beta_S \Delta T)$, we can calculate the temperature coefficient of Young's modulus of silicon to be $\beta_S = -70$ ppm K^{-1} . In earlier publications, the reported values vary from -55 to -113 ppm K^{-1} [26].

According to the measurements, the use of an ALD alumina coating on a silicon oscillator results in a decrease in the temperature sensitivity of the resonance frequency with increasing film thickness. For the oscillator with a 662 nm thick alumina coating, the temperature-induced drift in the resonance frequency was -24 ppm K^{-1} , which is 31% less than that of an uncoated silicon oscillator. A theoretical discussion given in [27] shows that, for thin coatings, the thermal drift in resonance frequency depends linearly on the ratio of thicknesses of the coating layer and the silicon oscillator. The temperature dependence of the elasticity of the ALD alumina was evaluated by using the measured data, as shown in figure 5, and linear approximations of $E_S = E_{S0}(1 + \beta_S \Delta T)$ and $E_A = E_{A0}(1 + \beta_A \Delta T)$ in equation (2). This approach results in a rather large positive value for the temperature coefficient of Young's modulus of the ALD alumina, $\beta_A = 1600 \pm 300$ ppm K^{-1} . Here, the thermal mismatch-based frequency drift is neglected because the silicon oscillators are uniformly coated on all sides and the difference in thermal expansion coefficients of silicon and ALD alumina is small ($\alpha_S = 3$ ppm K^{-1} [27], $\alpha_A = 5$ ppm K^{-1} [28]).

4.5. Reflectivity as a function of alumina film thickness

In many cases, only a few nanometer thick coating is enough for electrical insulation or mechanical protection whereas typical optical applications require the use of much thicker films. For example, in the case of an optical quarter wavelength film, the film needs to be tens or hundreds of nanometers thick. When light arrives at normal incidence to the planar interface of the two media with refractive indices n_1 and n_2 , the light experiences reflectivity R_{12} according to

$$R_{12} = \frac{(n_1 - n_2)^2}{(n_1 + n_2)^2}. \quad (4)$$

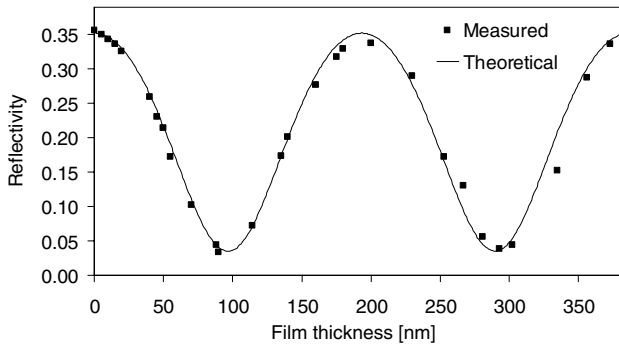


Figure 6. Reflectivity of the alumina-coated silicon oscillator at $\lambda = 633$ nm as a function of the film thickness. The refractive index of the ALD alumina film was $n = 1.64$. Measured data corresponds very well to the theoretical reflectivity calculated from equation (5).

If the substrate is coated with a thin film, the incident light undergoes multiple reflections at both interfaces. The relative phase between these reflections depends on the thickness d of the thin film. The total reflectivity at normal incidence can be written as

$$R_{\text{tot}} = \frac{R_{12} + R_{23} + 2\sqrt{R_{12}R_{23}} \cos\left(\frac{4\pi dn_2}{\lambda}\right)}{1 + R_{12}R_{23} + 2\sqrt{R_{12}R_{23}} \cos\left(\frac{4\pi dn_2}{\lambda}\right)}, \quad (5)$$

where R_{12} is the reflectivity at the boundary of the initial medium and the thin film and R_{23} is the reflectivity at the boundary of the thin film and the substrate. The symbol n_2 is the refractive index of the thin film. In this work, the reflectivity of each ALD alumina coating was determined by measuring the optical power of the incident HeNe-laser beam with a photodiode and comparing it with the optical power of the beam reflected from the alumina-coated silicon oscillator. The solid line in figure 6 illustrates the reflectivity of the alumina-coated silicon oscillator as a function of the film thickness calculated with equation (5). As shown in figure 6, the measured reflectivity with varying alumina film thickness corresponds very well to the calculated one.

A thin film serves as a single-layer anti-reflection coating if its refractive index is lower than that of the substrate. If the film thickness corresponds to the quarter of the wavelength of light (or any odd number of quarter wavelengths), the reflectivity is given by

$$R_{\text{AR}} = \left(\frac{n_1 n_3 - n_2^2}{n_1 n_3 + n_2^2}\right)^2, \quad (6)$$

where n_1 , n_2 and n_3 are the refractive indices of the initial medium, thin film and the substrate, respectively. One could even achieve no reflection at all if $n_2 = (n_1 n_3)^{1/2}$. In order to obtain this with a silicon substrate ($n_3 = 3.92$ at 633 nm), the refractive index of the thin film should be $n_{2,0} = 1.98$. In our case the refractive index of the ALD alumina ($n_2 = 1.64$) was somewhat lower, but still the reflectivity was reduced quite remarkably from $R_{\text{Si}} = 0.35$ for a clean silicon surface to $R_{\text{AR}} = 0.035$ for a quarter wavelength film-coated silicon surface.

5. Conclusions

In this work the influence of the ALD alumina thin films on the behavior of a high-*Q* mechanical silicon oscillator was

experimentally studied. It was demonstrated that alumina films with thicknesses up to 100 nm can be deposited on mechanical resonant components without degrading the intrinsic high mechanical quality. Alumina films effectively stiffen the resonant structures leading to the increase in the resonance frequency with increasing film thickness. The resonance frequency of the silicon oscillator was less sensitive to changes in ambient temperature if the oscillator was coated with alumina and the temperature sensitivity decreases as the film thickness increases. It was shown that alumina thin films on silicon substrates can be used as a single-layer anti-reflection coating, offering a significant reduction in the reflectivity from $R_{\text{Si}} = 0.35$ for a clean silicon surface to $R_{\text{AR}} = 0.035$ for a silicon surface with a quarter wavelength alumina coating at $\lambda = 633$ nm. The results of this work validate the high potential of resonant microstructures with ALD alumina thin films in high precision measurement and sensor applications.

Acknowledgment

This work has been supported by Tekes (Finnish Funding Agency for Technology and Innovation) grant no. 40322/05.

References

- [1] Stoldt C R and Bright V M 2006 Ultra-thin film encapsulation processes for micro-electro-mechanical devices and systems *J. Phys. D: Appl. Phys.* **39** R163–70
- [2] Hoivik N D, Elam J W, Linderman R J, Bright V M, George S M and Lee Y C 2003 Atomic layer deposited protective coatings for micro-electromechanical systems *Sensors Actuators A* **103** 100–8
- [3] Mayer T M, Elam J W, George S M, Kotula P G and Goeke R S 2003 Atomic-layer deposition of wear-resistant coatings for microelectromechanical devices *Appl. Phys. Lett.* **82** 2883–5
- [4] Eklund E J and Shkel A M 2005 Factors affecting the performance of micromachined sensors based on Fabry–Perot interferometry *J. Micromech. Microeng.* **15** 1770–6
- [5] Tripp M K, Stampfer C, Miller D C, Helbling T, Herrmann C F, Hierold C, Gall K, George S M and Bright V M 2006 The mechanical properties of atomic layer deposited alumina for use in micro- and nano-electromechanical systems *Sensors Actuators A* **130–131** 419–29
- [6] Copel M, Cartier E, Gusev E P, Guha S, Bojarczuk N and Poppeller M 2001 Robustness of ultrathin aluminum oxide dielectrics on Si(001) *Appl. Phys. Lett.* **78** 2670–2
- [7] Groner M D, Elam J W, Fabreguette F H and George S M 2002 Electrical characterization of thin Al₂O₃ films grown by atomic layer deposition on silicon and various metal substrates *Thin Solid Films* **413** 186–97
- [8] Gusev E P, Copel M, Cartier E, Baumvol I J R, Krug C and Gribelyuk M A 2000 High-resolution depth profiling in ultrathin Al₂O₃ films on Si *Appl. Phys. Lett.* **76** 176–8
- [9] Herrmann C F, DelRio F W, Bright V M and George S M 2005 Conformal hydrophobic coatings prepared using atomic layer deposition seed layers and non-chlorinated hydrophobic precursors *J. Micromech. Microeng.* **15** 984–92
- [10] Zhao Z W, Tay B K, Lau S P and Xiao C Y 2003 Microstructural and optical properties of aluminum oxide thin films prepared by off-plane filtered cathodic vacuum arc system *J. Vac. Sci. Technol. A* **21** 906–10

- [11] Mitchell D R G, Triani G, Attard D J, Finnie K S, Evans P J, Barbé C J and Bartlett J R 2006 Atomic layer deposition of TiO₂ and Al₂O₃ thin films and nanolaminates *Smart Mater. Struct.* **15** S57–64
- [12] Ott A W, Klaus J W, Johnson J M and George S M 1997 Al₂O₃ thin film growth on Si(100) using binary reaction sequence chemistry *Thin Solid Films* **292** 135–44
- [13] Hahtela O, Chekurov N and Tittonen I 2005 Non-tilting out-of-plane mode high-*Q* mechanical silicon oscillator *J. Micromech. Microeng.* **15** 1848–53
- [14] Dillon A C, Ott A W, Way J D and George S M 1995 Surface chemistry of Al₂O₃ deposition using Al(CH₃)₃ and H₂O in a binary reaction sequence *Surf. Sci.* **322** 230–42
- [15] Puurunen R L 2005 Surface chemistry of atomic layer deposition: a case study for the trimethylaluminum/water process *J. Appl. Phys.* **97** 121301
- [16] Meyer G and Amer N M 1988 Novel optical approach to atomic force microscopy *Appl. Phys. Lett.* **53** 1045–7
- [17] Meirovitch L 1967 *Analytical Methods in Vibrations* (New York: Macmillan)
- [18] Stoldt C R, Fritz M C, Carraro C and Maboudian R 2001 Micromechanical properties of silicon-carbide thin films deposited using single-source chemical-vapor deposition *Appl. Phys. Lett.* **79** 347–9
- [19] Wang K, Wong A-C and Nguyen C T-C 2000 VHF free-free beam high-*Q* micromechanical resonators *J. Microelectromech. Syst.* **9** 347–60
- [20] Yasumura K Y, Stowe T D, Chow E M, Pfafman T, Kenny T W, Stipe B C and Rugar D 2000 Quality factors in micron- and submicron-thick cantilevers *J. Microelectromech. Syst.* **9** 117–25
- [21] Buser R A and de Rooij N F 1990 Very high *Q*-factor resonators in monocrystalline silicon *Sensors Actuators A* **21–23** 323–7
- [22] Sandberg R, Molhave K, Boisen A and Svendsen W 2005 Effect of gold coating on the *Q*-factor of a resonant cantilever *J. Micromech. Microeng.* **15** 2249–53
- [23] Hahtela O, Nera K and Tittonen I 2004 Position measurement of a cavity mirror using polarization spectroscopy *J. Opt. A: Pure Appl. Opt.* **6** S115–20
- [24] Stemme G 1991 Resonant silicon sensors *J. Micromech. Microeng.* **1** 113–25
- [25] Sandberg R, Svendsen W, Molhave K and Boisen A 2005 Temperature and pressure dependence of resonance in multi-layer microcantilevers *J. Micromech. Microeng.* **15** 1454–8
- [26] Tudor M J, Andres M V, Foulds K W H and Naden J M 1988 Silicon resonator sensors: interrogation techniques and characteristics *IEE Proc.* **135** 364–8
- [27] Shen F, Lu P, O'Shea S J, Lee K H and Ng T Y 2001 Thermal effects on coated resonant microcantilevers *Sensors Actuators A* **95** 17–23
- [28] Zhang Y, Dunn M L, Gall K, Elam J W and George S M 2004 Suppression of inelastic deformation of nanocoated thin film microstructures *J. Appl. Phys.* **95** 8216–25